

Human fragmentation effects are genetically detectable after 6 years in the island-endemic *Primulina heterotricha* (Gesneriaceae)

Wen-Ting Jin¹, Shao-Jun Ling¹, Myong Gi Chung², Mi Yoon Chung³, Jordi López-Pujol⁴, and Mingxun Ren¹

¹Hainan University

²Gyeongsang National University Division of Life Sciences

³Chungnam National University

⁴Institut Botanic de Barcelona

November 1, 2023

Abstract

Anthropogenic disturbances have long been acknowledged to be one of the primary threats to biodiversity worldwide, while little is still understood about how human-built infrastructure affects the gene flows and phylogeographic structure of plants. Such information is helpful for the conservation and restoration of human-disturbed ecosystems. Here we studied effects of a big river with a huge reservoir and two expressways on an island-endemic *Primulina heterotricha* (Gesneriaceae) on Hainan Island, China, one of the key parts of the globally important Indo-Burma biodiversity hotspot. By applying comparative phylogeography using one nuclear ribosomal DNA and two chloroplast DNA sequences, we estimated the levels of genetic diversity and differentiation in 176 and 117 individuals collected, respectively, before (in 2016) and after (in 2022) the construction of two expressways in Hainan Island, from the same eight populations of *P. heterotricha*. We found that *Primulina heterotricha* significantly increased nuclear genetic differentiation during the period 2016–2022, which coincides with the opening of the two expressways. Also notably, the sharing of ribotypes among the three groups of populations separated by the expressway network almost disappeared for the same period. Moreover, the changes in the significance of genetic barriers before and after road construction suggest that geographic isolation caused by both the reservoir and the expressways is key for understanding the present phylogeographical patterns of *P. heterotricha*. We provide direct evidence that anthropogenic infrastructures such as reservoirs and expressways have been capable of increasing genetic differentiation and, thus, modifying the phylogeographical pattern of *P. heterotricha*, in just a six-year period (or two generations of the study plant). To mitigate such negative pressure, we suggest establishing ecological corridors to enhance gene exchange between the two sides of the anthropogenic barriers.

Research Article

Human fragmentation effects are genetically detectable after 6 years in the island-endemic *Primulina heterotricha* (Gesneriaceae)

Wen-Ting Jin^{1,2,#} | Shao-Jun Ling^{1,2,#} | Myong Gi Chung³ | Mi Yoon Chung⁴ | Jordi López-Pujol^{5,6} | Ming-Xun Ren^{1,2,*}

¹Key Laboratory of Agro-Forestry Environmental Processes and Ecological Regulation of Hainan Province, Hainan University, Haikou 570228, China

²Center for Eco-Environment Restoration Engineering of Hainan Province, Hainan University, Haikou 570228, China

³Division of Life Science and RINS, Gyeongsang National University, Jinju, 52828, South Korea

⁴Department of Biological Sciences, Chungnam National University, Daejeon 34134, South Korea

⁵Botanic Institute of Barcelona, CSIC-Ajuntament de Barcelona, Barcelona 08038,
Spain

⁶Escuela de Ciencias Ambientales, Universidad Espíritu Santo (UEES), Samborondón 091650, Ecuador

These authors contributed equally

*Correspondence: Ming-Xun Ren, Email:renmx@hainanu.edu.cn

Running title : Plant phylogeography and human barriers

Data Availability Statement: The data as supporting material are provided as a file with the name of ‘Supporting Information for review and publication’.

Acknowledgements:

This study was supported by a grant from the National Natural Science Foundation of China (42371054, 41871041), Fund for young scholars of Hainan Natural Science Foundation (422QN269), Hainan Postdoctoral Research Project (2022-BH-22), Hainan Provincial Innovative Research Projects of Postgraduates (No. Qhys2022-74).

Abstract

Anthropogenic disturbances have long been acknowledged to be one of the primary threats to biodiversity worldwide, while little is still understood about how human-built infrastructure affects the gene flows and phylogeographic structure of plants. Such information is helpful for the conservation and restoration of human-disturbed ecosystems. Here we studied effects of a big river with a huge reservoir and two expressways on an island-endemic *Primulina heterotricha* (Gesneriaceae) on Hainan Island, China, one of the key parts of the globally important Indo-Burma biodiversity hotspot. By applying comparative phylogeography using one nuclear ribosomal DNA and two chloroplast DNA sequences, we estimated the levels of genetic diversity and differentiation in 176 and 117 individuals collected, respectively, before (in 2016) and after (in 2022) the construction of two expressways in Hainan Island, from the same eight populations of *P. heterotricha*. We found that *Primulina heterotricha* significantly increased nuclear genetic differentiation during the period 2016–2022, which coincides with the opening of the two expressways. Also notably, the sharing of ribotypes among the three groups of populations separated by the expressway network almost disappeared for the same period. Moreover, the changes in the significance of genetic barriers before and after road construction suggest that geographic isolation caused by both the reservoir and the expressways is key for understanding the present phylogeographical patterns of *P. heterotricha*. We provide direct evidence that anthropogenic infrastructures such as reservoirs and expressways have been capable of increasing genetic differentiation and, thus, modifying the phylogeographical pattern of *P. heterotricha*, in just a six-year period (or two generations of the study plant). To mitigate such negative pressure, we suggest establishing ecological corridors to enhance gene exchange between the two sides of the anthropogenic barriers.

KEYWORDS

Anthropogenic disturbances, gene flow, Hainan Island, Island biogeography

1 | INTRODUCTION

Human activities, which are regarded as primary threats to biodiversity worldwide, are capable of disturbing the habitat integrity and, thus, modifying phylogeographic patterns of naturally distributed species (Young et al., 1996; Aguilar et al., 2006; Martínez-Ramos et al., 2016). For example, anthropogenic infrastructures such as expressways, buildings, and expansive farmlands can interrupt plant pollination and seed dispersal by hindering the movements and migration of insects and other animals (Honnay & Jacquemyn, 2007). Fragmentation of natural populations and geographical isolation of individuals may also lead to increased

levels of inbreeding and genetic drift (Lowe et al., 2015), putting populations at risk of extinction (Tambarussi et al., 2017; Moraes et al., 2018).

Hainan Island, located in south China, has an area of 35,000 km² and is a distinctive part of the globally important Indo-Burma biodiversity hotspot (Myers et al., 2000), as it harbors *ca.* 4800 vascular plants in total with nearly 500 endemics (Francisco-Ortega et al., 2010a, b; Yang, 2013). Most of this rich plant diversity (e.g. 80% of the endemic species) are concentrated in the south-central mountain system of the island (Francisco-Ortega et al., 2010a, b). Notably, this area is the home to the world’s most endangered primate *Nomascus hainanus* Thomas (Long et al., 2021), highlighting its conservation value.

Currently, however, Hainan island is experiencing a rapid economic development, which is partly based on the construction of large infrastructures; for example, the local authorities are aiming to build the world’s biggest free trade port (www.xinhuanet.com/english/2018-04/13/c_137109243.htm). The landscapes and vegetation have been severely affected in the past decades due to the accelerated growth of the human population and urbanization. For example, the Daguangba Reservoir on the Changhua River, the second largest river on the island, was completed in 1994 and formed a sluggish waterbody of nearly 6 km in width. This huge reservoir located between Mt. E’xian and Mt. Jianfeng may disrupt the connectivity of the natural vegetation of these two mountains. Moreover, two expressways were recently built in Hainan’s biodiversity-rich mountainous regions: Road G9811 (hereafter referred to as Expressway 1) was completed in 2018 and has a width of 26 m, and Road S10 (hereafter referred to as Expressway 2) was built in 2019 and is 20 m wide (www.xinhuanet.com/english/2021-04/15/c_139882827.htm). These anthropogenic constructions lie in the middle part of the south-central mountains on the island and may affect habitat integrity and genetic continuity of the rare and endangered plants, which may further result in the alteration of evolutionary processes, especially genetic differentiation and the whole plant’s phylogeographical structure.

The family Gesneriaceae on Hainan Island is notable for its high levels of species diversity and endemism (Wei, 2010; Ling et al., 2017a, b). Fourteen genera and 25 species of the family occur on the island, including one endemic genus and 10 endemic species (Li & Wang, 2005; Yang, 2013; Ling et al., 2017a, 2020b). *Primulina heterotricha* (Merr.) Y. Dong & Yin Z. Wang, one of these endemic species, is widely distributed in the south-central mountains on the island (Ling et al., 2017a, b). The plant, a short-lived herb (with a generation time of 1–3 years), has zygomorphic tubular flowers that are pollinated by several insects, particularly *Glossamegilla malaccensis* Friese and *G. yunnanensis* Wu of Anthophoridae (Ling, 2017a, b). The fruit (capsule) is erect with small brown and fusiform-shaped seeds, suggesting a poor dispersal capability that is likely associated with water courses (MXR, personal observations). Taking all the above-mentioned factors into consideration, this species is a good model system to uncover possible short-term fragmentation effects of the Daguangba Reservoir and the newly-built expressways on its genetic differentiation and phylogeographical patterns.

In this study, we addressed the following questions: (1) are the recently built reservoir and expressways (i.e. artificial barriers) already influencing the genetic make-up in the Hainan-endemic *P. heterotricha*? and (2) if yes, how are these artificial barriers affecting the population differentiation and phylogeographical patterns of the study species? To get insights into these questions, we performed a population genetics and a phylogeographical study based on samples of *P. heterotricha* that were collected in 2016 and 2022 (i.e., before and after expressway construction), using conserved and slowly evolving nuclear and chloroplast DNA sequences.

2 | Materials and methods

2.1 | Sample collection and laboratory procedures

Eight populations roughly covering the whole distribution range of *Primulina heterotricha* were sampled, and included BW (Mt. Bawang), YJ (Mt. Yajia), EX (Mt. Erxian), YG (Mt. Yingge), QX (Mt. Qixian), WZ (Mt. Wuzhi), XA (Xian’an Stone Forest), and JF (Mt. Jianfeng) (Table 1; Figure 1). A total of 176 samples were collected in 2016 and 117 samples in 2022 (Table 1). Although we did not sample prior to 1994 when the Daguangba Reservoir on the Changhua River was completed, sampling from the eight populations before (2016) and after (2022) the construction of the two expressways (expressways 1 and 2 were completed

in 2018 and 2019, respectively) would allow us to detect possible genetic and phylogeographic effects of habitat fragmentation. Distance between populations ranged from 6 to 72 km, and the elevation of collected populations varied from 600 (YG) to 1163 m (YJ) above sea level (Table 1). Considering the physical barriers posed by the two expressways and the dam, the populations can be tentatively divided into four groups: the northwest (NW) group of populations (i.e. BW, YJ, EX, and YG), the southeast (SE) group (QX and WZ), the southern (S) group (XA), and the southwest (SW) group (JF). In each population, fresh leaf samples were collected from individuals at least 10 m apart. Each sampled leaf was dried quickly in a separate plastic bag containing 20 to 30 g of silica gel and stored at -80 later.

Table 1 Basic information of eight studied populations of *Primulina heterotricha* on Hainan Island.

Sampling site	Population code	Coordinates	Elevation (m)	Sampling size	
				Year 2016	Year 2022
Mt. Bawang	BW	N19°07'13.46"/E109°09'36.73"	1163	16	16
Mt. Yajia	YJ	N19°04'34.57"/E109°08'50.35"	1163	16	15
Mt. Exian	EX	N19°09'18.22"/E109°06'35.41"	902	31	16
Mt. Yingge	YG	N19°01'27.15"/E109°03'11.65"	600	9	10
Mt. Qixian	QX	N18°43'10.48"/E109°02'00.05"	1163	30	15
Mt. Wuzhi	WZ	N18°53'55.00"/E109°05'52.00"	1163	25	15
Mt. Xianan	XA	N18°53'39.28"/E109°02'25.82"	978	16	15
Mt. Jianfeng	JF	N18°46'11.14"/E108°51'57.57"	808	33	15
Sum				176	117

Total genomic DNA for all samples was extracted using the standard CTAB procedure (Doyle & Doyle, 1987) from 30 mg of dried leaf tissue, and served as the template for the polymerase chain reaction (PCR). DNA quality and quantity were determined on 0.8% agarose gels stained with 2.5 μ L Goldview (Aidlab Biotechnologies Co., Ltd., Beijing, China), with AL2000 DNA marker (Aidlab Biotechnologies).

One nuclear ribosomal DNA (nrDNA) sequence, the ribosomal inter-transcribed spacer (ITS) region comprising spacer 1, the 5.8S ribosomal gene and spacer 2 (White et al., 1990), and the two chloroplast DNA (cpDNA) intron-spacer regions *trn L-trn F* (Taberlet et al., 1991) and *yef 1b* (Dong et al., 2015), were used in this study (Table 2). PCR reactions were set up in a volume of 25 μ L, composed of 20 μ L ddH₂O, 2.5 μ L 10 \times buffer, 0.5 μ L 10 mM dNTPs, 0.5 μ L each 5 μ M primer, 0.5 μ L DNA template and 0.5 μ L 5 U/ μ L Taq polymerase (Aidlab Biotechnologies). The PCR reactions were carried out on a 2720 Thermal Cycler (Applied Biosystems by Life Technologies, Singapore). The PCR program for ITS1/2 and *trn L-trn F* was designed with an initial denaturation of 5 min at 94 $^{\circ}$ C, followed by 35 cycles of 1 min at 94 $^{\circ}$ C, 1 min at 55 $^{\circ}$ C, 1 min at 72 $^{\circ}$ C, and with a final extension of 10 min at 72 $^{\circ}$ C. Amplification of *yef 1b* used the following protocol: 4 min at 94 $^{\circ}$ C, 35 cycles of 30 s at 94 $^{\circ}$ C, 40 s at 58 $^{\circ}$ C, and 1 min at 72 $^{\circ}$ C, ending with 10 min at 72 $^{\circ}$ C. All the PCR products were verified based on size by gel electrophoresis. The amplicons were sequenced by an ABI 3730 DNA Analyzer in forward and reverse directions based on the BigDye Terminator Cycle Sequencing Ready Kit (Applied Biosystems, Foster City, CA, U.S.A.) in BGI (Beijing Genomics Institute, China).

2.2 | Genetic diversity

The chromatograms from both directions of the ITS1/2 and cpDNA sequences were checked visually and edited manually with the software BioEdit (Hall, 1999) for base confirmation and contiguous sequence editing; each base/character was equally weighted before analysis, and each indel/gap was represented as a single mutation. Three sequences were manually aligned and trimmed integrally where necessary using MEGA v.6.5 (Kumar et al., 2008) separately. The two no-coding cpDNA sequences were assembled as a single locus for subsequent analysis by SequenceMatrix v.1.7.8 (Vaidya et al., 2011), and the partition homogeneity test

of cpDNA sequences vs. nrITS sequences was carried out with PAUP* v.4.0a164 (Swofford, 2002). Since non-homogeneity of both matrices was detected, nrITS and cpDNA were analyzed independently.

DNASP v.6.12.01 (Rozas et al., 2017) was used to compute the number of identified ribotypes/chlorotypes (Nn), haplotype diversity (h) within populations, polymorphic sites (S), nucleotide diversity (π), and the average number of nucleotide differences (Nd) separately for nrITS and cpDNA matrices. The geographic distribution maps of ribotypes/chlorotypes at the population level, also separately for nrITS and cpDNA sequences, were constructed and visualized with ArcGIS v.10.8 (ESRI, Redlands, CA, U.S.A.).

2.3 | Phylogenetic relationships

We inferred the optimal model of nucleotide substitution using MrModeltest v.2.3 (Nylander, 2004), based on the AIC (Akaike Information Criteria) (Akaike, 1981). The putative most suitable model (GTR+I+G) was used in inferring the phylogenetic relationships of the identified ribotypes, which was done through maximum likelihood (ML) and Bayesian inference (BI) trees (Gao et al., 2015; Genbank with accession number DQ872827). ML analysis of ribotypes was conducted using MEGA v.6.5 with the optimal substitution model and 1000 bootstrap replicates carried out to assess the support of the resulting groups. BI analysis of ribotypes was conducted using MrBayes v.3.2.6 (nst = 2, rates = equal) (Ronquist et al., 2012), using the optimal model of nucleotide substitutions inferred by AIC in PAUP v.4.0a164. The analysis began with a random tree using Markov Chain Monte Carlo (MCMC) chains with 10 million generations, sampling every 10,000 generations across four independent Bayesian runs. The first 2500 trees (25% of total trees) were discarded as burn-in, and the remaining trees were summarized in a 50% majority-rule consensus tree with the posterior probabilities (PP). Chain convergence was assessed by checking the effective sample size that was bigger than 200 for each parameter in Tracer v.1.6 (Rambaut & Drummond, 2007), and the length and PP of each branch were visualized by FIGTREE v.1.4.2 (Rambaut, 2009).

2.4 | Population structure, mismatch distribution analysis, and neutrality detection

The population structure of nrDNA and cpDNA sequences was inferred using the Bayesian clustering procedure implemented in STRUCTURE v.2.3.4 (Evanno et al., 2005) without prior structure information; this software identifies the most probable number (K) of genetic clusters of origin of the sampled individuals and assigns individuals to clusters. We used MCMC iterations as implemented in STRUCTURE to explore the parameter space considering individual memberships to K clusters, ranging from $K = 1$ (null hypothesis of panmixia) to $K = 8$ (the total number of populations sampled). Three independent runs were performed with an admixture model at 10^5 MCMC iterations and a 10^5 burn-in period. The most likely number of population groups (K , indicating the number of true clusters in the data) and the model values (ΔK , according to the second-order rate of change of cluster K that best fits the data) were calculated in STRUCTURE HARVESTER (Earl & vonHoldt, 2012). The graphical representation of results was performed in the CLUMPAK server (<http://clumpak.tau.ac.il/index.html>).

An analysis of molecular variance (AMOVA) was conducted on nrDNA and cpDNA sequences separately to test genetic differentiation within populations, among groups, and populations within groups using GenAlEx v.6.503 (Peakall & Smouse, 2012). Population pairwise F_{ST} was measured using DNASP v.6.12.01, and population pairwise geographic distances were calculated by GenAlEx. To test whether there was local genetic variation attributable to isolation-by-distance among populations, the estimates of $F_{ST}/(1-F_{ST})$ and the corresponding natural logarithm of geographic distances (in km) between all pairwise combinations of the eight populations were regressed and subjected to a Mantel test (Mantel, 1967) with 999 random permutations in GenAlEx.

The genealogical relationships between ribotypes/chlorotypes based on the Medium-Joining model were inferred using NETWORK v.4.6.1.0 (<http://www.fluxus-engineering.com/>). To identify and quantify potential genetic discontinuities and biogeographic boundaries acting as major genetic barriers among *P. heterotricha* populations from both nrITS and cpDNA datasets, we calculated the Monmonier's maximum-difference algorithm in Barrier v.2.2 (Manni et al., 2004). The robustness of these barriers was assessed by bootstrapping genetic distances.

In order to detect possible recent range expansions, Tajima’s D (Tajima, 1989) and Fu’s F_s (Fu, 1997) were calculated to test the deviations from the null hypothesis of constant population size and neutral evolution for each DNA fragment. Pairwise mismatch distribution and neutrality tests for all populations were conducted in DNASP using the nrITS and cpDNA datasets separately.

3 | Results

3.1 | nrITS and cpDNA datasets

For the samples of 2016, the ITS1/2 sequence matrix comprised 701 bp in total, harbored 13 polymorphic sites (S) and 10 ribotypes (Nn) from 176 samples (Table 2). At the species level, the ITS1/2 nucleotide diversity (π) was 0.00435, the average number of nucleotide differences (Nd) was 2.988, and haplotype diversity (h) was 0.809 (Table 2). The geographical distribution of ribotypes showed that R1, R5, and R6 occurred in more than one population. R1 ribotype was shared by BW, YJ, EX, and QX, R5 was shared by QX and WZ, and R6 was shared by YG, WZ, and XA. The other seven ribotypes were private (Table 3; Figure 1a).

Table 2 Primer polymorphic sites (S), number of ribotypes/chlorotypes (Nn), haplotypes diversity (h), nucleotide diversity

DNA fragment

S

Nn

h

π

Nd

Fragment size

Tajimas’ D

Fu’s F_s

For the 2022 samples, the ITS1/2 sequence matrix comprised 640 bp in total (Table 2). Twenty-six S were present, which allowed the identification of 18 different ribotypes from a size of 117 samples (Table 2). At the species level, π was 0.00464, Nd was 2.912, and h was 0.876 (Table 2). Two ribotypes, R1 and R11, were shared by at least two populations (R1 was present in BW, YJ, and EX, and ribotype R11 occurred in YG and WZ). The other 16 ribotypes were private (Table 3; Figure 1b). Comparing samples between 2016 and 2022, there was a decrease in both the number (three in 2016 to two in 2022) and the percentage of shared ribotypes (30.0% in 2016 and 11.1% in 2022) (Table 3). Notably, the sharing of ribotypes among the three groups of populations separated by the expressway network (NW, S, and SE) is much diminished; while in 2016 R1 and R6 were shared by NW and SE, and R6 shared by NW, S, and SE, in 2022 only R11 was shared by NW and SE (Figure 1b).

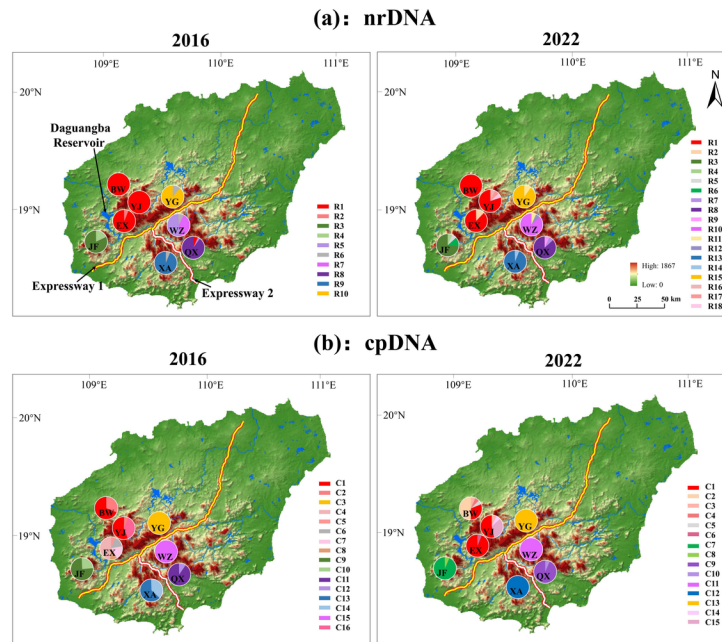


Figure 1 Haplotype distribution of (a) nrDNA ITS and (b) cpDNA *trn* L-F and *ycf* 1b in the years of 2016 and 2022 of eight populations of *Primulina heterotricha* on Hainan Island, south China.

The total length of the combined chloroplast alignments in 2016 was 1405 bp (730 bp and 674 bp in size for *trn* L-*trn* F and *ycf* 1b, respectively). The alignment contained 48 *S*, and 16 chlorotypes (*Nn*) were present among the 176 samples (Table 2). At the species level, π was 0.00940, *Nd* was 12.725, and *h* was 0.907 (Table 2). Of the 16 chlorotypes, only two (C1 and C2) were shared between populations (BW and YJ). The other 14 chlorotypes were private (Table 3; Figure 1c). For the 2022 samples, the combined alignment of two cpDNA regions comprised 1592 bp (870 bp and 722 bp in size for *trn* L-*trn* F and *ycf* 1b, respectively) which contained 42 *S*, and 15 *Nn* were present among the 117 samples (Table 2). At the species level, π was 0.00868, *Nd* was 13.637, and *h* was 0.874 (Table 2). Of the 15 chlorotypes, only two (C1 and C3) were shared (C1 was shared by BW, YJ, and EX, and C3 by BW and YJ) (Table 3). The other 13 chlorotypes were private (Table 3; Figure 1d). In sum, and contrary to the ITS, there were no major differences between the 2016 and 2022 cpDNA datasets, with the same number (two) and almost the same percentage (12.5% vs. 13.3%) of shared chlorotypes, all occurring on the NW group of populations.

Table 3 Nucleotide/haplotype information from nrDNA and cpDNA of eight populations of *Primulina heterotricha* on Hainan Island in 2016 and 2022. Private ribotypes/chlorotypes (occurring in only one population) are given in **bold**.

Population	2016 Type (no. of individuals)	2016 <i>h</i>	2016 π	2022 Type (no. of individuals)
ITS	ITS	ITS	ITS	ITS
BW	R1(16)	0	0	R1(16)
YJ	R1(16)	0	0	R1(12), R16(1) , R17(3)
EX	R1(29), R2(2)	0.1247	0.00018	R1(14), R2(2) , R3(13)
YG	R6(1), R10(8)	0.2222	0.00032	R11(1), R15(9) , R18(5)
QX	R1(2), R5(1), R8(27)	0.1908	0.00064	R7(1) , R8(13) , R9(13)

WZ	R5(13), R6(2), R7(10)	0.5867	0.00285	R10(13) , R11(1), R12(1)
XA	R6(1), R9(15)	0.1250	0.00036	R13(14) , R14(1)
JF	R3(27) , R4(6)	0.3068	0.00044	R3(11) , R4(1) , R5(1)
Sum		1.5562	0.00479	
<i>trnL-F</i> and <i>ycf1b</i>	<i>trnL-F</i> and <i>ycf1b</i>	<i>trnL-F</i> and <i>ycf1b</i>	<i>trnL-F</i> and <i>ycf1b</i>	<i>trnL-F</i> and <i>ycf1b</i>
BW	C1(11), C2(5)	0.4583	0.00033	C1(5), C2(8) , C3(1)
YJ	C1(9), C2(1), C16(6)	0.5750	0.00082	C1(8), C3(1), C14(1)
EX	C4(15) , C5(2) , C6(5) , C7(6) , C8(3)	0.7118	0.00380	C1(15), C6(1)
YG	C3(9)	0	0	C13(10)
QX	C11(27) , C12(3)	0.1862	0.00027	C9(14) , C10(1)
WZ	C15(25)	0	0	C11(15)
XA	C13(10) , C14(6)	0.5000	0.00074	C12(15)
JF	C9(25) , C10(8)	0.3788	0.00028	C7(14) , C8(1)
Sum		2.8101	0.00624	

3.2 | Phylogenetic relationships

For samples of 2016, the network separated the 10 ribotypes of the nuclear ITS into three different monophyletic lineages. Clearly, the ribotypes R1, R2, R6, and R10 that are present in the northwest (NW) group of populations formed a clade; R5 and R7–R9 dominating the south (S) and southeast (SE) populations had the closest phylogenetic relationship to the NW clade, while the R3 and R4 ribotypes that are exclusive to the southwest (SW) populations formed an independent clade from the NW one (Figure 2a). Similarly, for the 2022 samples, the network separated the 18 ribotypes of the nuclear ITS into three monophyletic lineages. The ribotypes R1, R2, R11, R15–R17, and R18, which are dominating the NW populations, converged into a group, R7–R10 and R12–R14 from the S and SE groups showed the closest phylogenetic relationship, and R3–R5, and R6, which are exclusive to the SW group, formed an independent clade (Figure 2c). In addition, BI and ML trees with high PP/BS values based on the ribotypes showed very similar results (Figures 2a, 2c).

Regarding the cpDNA, the pattern of phylogenetic relationships was very close to that of nrDNA. For both sampling periods (2016 and 2022), the network of chlorotypes showed three monophyletic lineages (Figures 2b, 2d). The chlorotypes most abundant in the NW group of populations (C1–C8 and C16 in 2016; C1–C6, C13, C14, and C15 in 2022) formed a clade, which was closest to the clade formed by the chlorotypes from the S and SE group of populations (C12–C15 in 2016, C9–C12 in 2022); the clade formed by the chlorotypes exclusive to the SW group (population JF; C9 and C10 in 2016, C7 and C8 in 2022; Figures 2b, 2d) was the most distant with respect to the NW one. Again, BI and ML trees with high BS/PP values based on chlorotypes showed very similar results (Figures 2b, 2d).

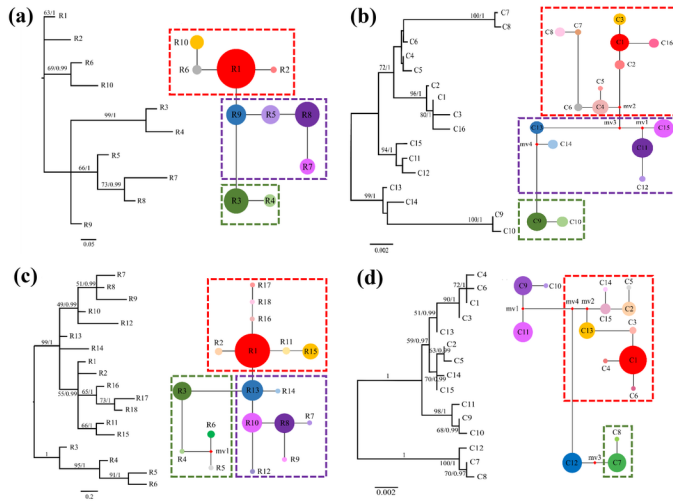


Figure 2 Phylogenetic trees and networks showing genetic relationships among observed ITS ribotypes in (a) 2016 and (c) 2022 and *trn* L-F and *ycf* 1b chlorotypes in (b) 2016 and (d) 2022 of *Primulina heterotricha* populations. The relative sizes of the circles in the network are proportional to the haplotype frequencies, and missing haplotypes are represented by a small red spot. The frames indicate different clades.

3.3 | Population genetic structure and phylogeographical patterns

The pairwise genetic differentiation (F_{ST}) was low for the nrITS dataset: for the 2016 samples, F_{ST} values ranged from 0 (BW-EX and YJ-EX pairs) to 0.010 (JF-YG and JF-WZ pairs) with a mean of 0.0045; estimates for the 2022 samples ranged from 0 (BW-EX pair) to 0.013 (JF-YG), averaging 0.0054 (Table S1). Regarding the cpDNA dataset, F_{ST} values for 2016 samples ranged from 0.001 (BW-YJ pairs) to 0.020 (JF-EX and JF-YG pairs), with a mean of 0.0098, while values for the 2022 samples ranged from 0.001 (JF-XA pair) to 0.018 (EX-XA, EX-JF, OX-XA, OX-JF, WZ-XA, and WZ-JF pairs), averaging 0.0097 (Table S2). The population that is separated from the rest by the dam (JF) showed the largest pairwise F_{ST} values for both datasets, although for the cpDNA the population XA also showed relatively high levels of genetic divergence (Tables S1, S2). Indeed, mean F_{ST} values between populations belonging to different groups were considerably higher when separated by the dam, i.e. JF (= SW region) vs. NW region, than when separated by expressways (the rest of pairwise values; Tables S3, S4); for nrDNA, $F_{ST-dam[2022]} = 0.0113 \pm 0.0013$ and $F_{ST-dam[2016]} = 0.0085 \pm 0.001$ vs. $F_{ST-expwy[2022]} = 0.0075 \pm 0.0017$ and $F_{ST-expwy[2016]} = 0.0062 \pm 0.0020$; for cpDNA, $F_{ST-dam[2022]} = 0.0170 \pm 0.0008$ and $F_{ST-dam[2016]} = 0.0193 \pm 0.0010$ vs. $F_{ST-expwy[2022]} = 0.0110 \pm 0.0077$ and $F_{ST-expwy[2016]} = 0.0122 \pm 0.0030$. Thus, as also occurred among individual populations, F_{ST} values among groups of populations increased during the period 2016–2022 only for nrITS.

Based on the ΔK approach, $K = 3$ was the most likely number of genetic clusters after running the software STRUCTURE (Figures S1a, S1b), both for the 2016 and 2022 datasets of nrDNA. In the $K = 3$ grouping scheme, one cluster included the BW, YJ, EX, and YG populations, which represent the NW group of populations (Figures 3a, 3b). The SE group of populations (QX and WZ) formed another cluster, while the

XA population showed two genetic components (NW and SE, with NW decreasing rapidly its weight from 2016 to 2022). The population JF constituted the third cluster.

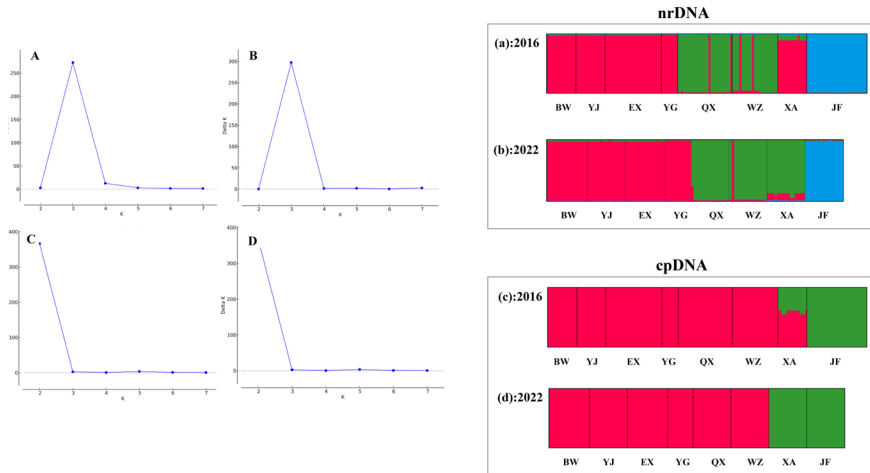


Figure 3 Results of STRUCTURE based on nrDNA and cpDNA samples of *Primulina heterotricha* populations collected in 2016 and 2022.

The Bayesian clustering using cpDNA sequences was somewhat different compared to the nrDNA (Figures 3c and 3d), as there were only two genetic clusters ($K = 2$) (Figures S1c, S1d), suggesting that the dam acts as the main genetic barrier in both datasets. The first cluster included all the populations except JF (i.e., group SW) and partially XA (i.e., group S) for the 2016 dataset, while six years later the population XA fell within the second cluster.

AMOVA results showed that most ITS genetic variation resides among the four regions (Table 4), although this component declined from 71% (2016) to 62% (2022), and the within-population component increased from 9% (2016) to 16% (2022). CpDNA genetic variation residing among regions increased from 2016 (72%) to 2022 (90%), and, unlike the nrDNA, the within-population component decreased from 10% (2016) to 4% (2022).

Table 4 AMOVA of genetic variation of eight populations from four regions of *Primulina heterotricha* based on nrDNA and cpDNA in the years of 2016 and 2022.

ITS Year 2016	ITS Year 2016	Degree of freedom	Sum of squares	Estimated Variation	Variation (%)
	Among regions	3	371.793	2.617	71%
	Among pops	4	56.858	0.751	20%
	Within pops	168	55.099	0.328	9%
	Total	175	483.750	3.66	100%

Year 2022	Year 2022	Year 2022	Year 2022	Year 2022	Year 2022
	Among regions	3	218.566	2.310	62%
	Among pops	4	50.063	0.832	22%
	Within pops	109	65.133	0.598	16%
	Total	116	333.752	3.739	100%
cpDNA Year 2016	cpDNA Year 2016				
	Among regions	3	1313.175	9.308	72%
	Among pops	4	192.434	2.412	18%
	Within pops	168	210.613	1.254	10%
	Total	175	1716.222	12.974	100%
Year 2022	Year 2022	Year 2022	Year 2022	Year 2022	Year 2022
	Among regions	3	998.455	12.328	90%
	Among pops	4	52.041	0.868	6%
	Within pops	109	62.529	0.574	4%
	Total	116	1113.026	13.770	100%

3.4 | Geographical barrier, isolation by distance, mismatch distribution analysis, and neutrality detection

By calculating Monmonier's maximum difference using the program BARRIER, we found three obvious geographic barriers using nrDNA and cpDNA separately. For the 2016 samples, the first barrier using nrDNA (supported by 99% of F_{ST} matrices) separated QX from WZ and XA, thus partially corresponding to Expressway 2 (Figure 4a). The second barrier (66% support) separated the NW group from the other populations, thus fitting well the Daguangba Reservoir and Expressway 1. Finally, the third barrier (33% support) was found between populations XA and WZ (Figure 4a). For the 2022 samples, the first barrier (99% support) separated the JF population from the rest (i.e., the Daguangba Reservoir plus a section of Expressway 1) (Figure 4b). Part of the second (66% support) and third (33% support) barriers could also be assigned to some sections of expressways 1 and 2, respectively (Figure 4b).

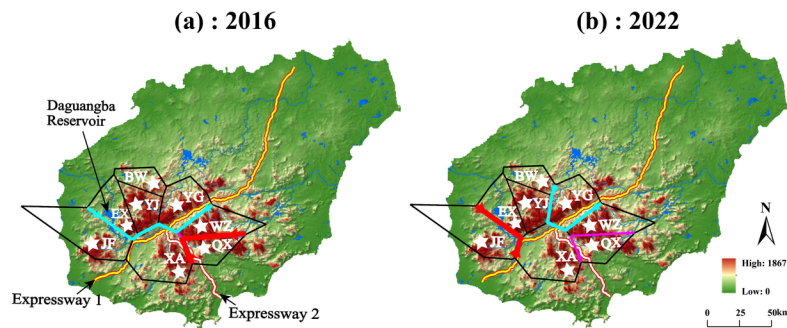


Figure 4 Genetic barriers obtained from BARRIER analysis based on nrDNA in the years of (a) 2016 (note the third barrier indicated by the faint purple line between XA and WZ) and (b) 2022 of *Primulina heterotricha* populations. Delaunay triangulation (black lines) and the bold lines (red, blue, and purple lines) indicate detected genetic barriers.

The barrier calculation based on the cpDNA sequence matrix showed similar patterns to those obtained with nrDNA. For the 2016 samples, the only difference was the location of the third barrier, which for the

cpDNA separated YJ from BW and YG (Figure 5a). For the 2022 samples, the first barrier changed to be the reservoir but also included some sections of expressways 1 and 2 (Figure 5b). The second barrier corresponded well to the section of Expressway 1 lying between YG and WZ, while the third barrier was located between YJ and YG (Figure 5b).

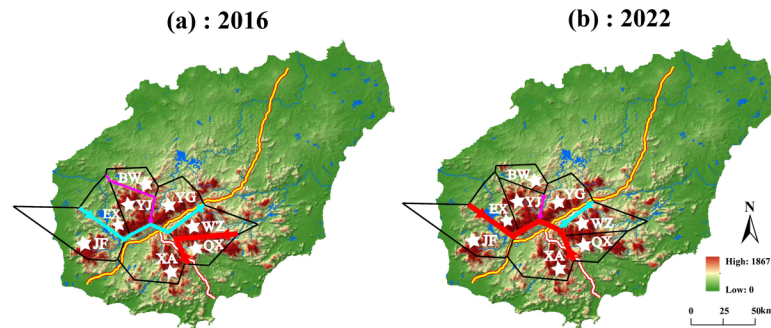


Figure 5 Genetic barriers obtained from BARRIER analysis based on cpDNA in the years of (a) 2016 and (b) 2022 of *Primulina heterotricha* populations. Delaunay triangulation (black lines) and inferred barriers (red, blue, and purple lines) separating the different original regions which show the geographic location of the genetic barrier.

The Mantel test showed a significant positive correlation between pairwise genetic distance and geographic distance for both nrDNA and cpDNA for the two study periods (Figure S2). The results of Tajima's D test and Fu's F_s test are presented in Table 2 with the associated simulated P -values. The values for D and F_s were positive for 2016 nrDNA sequences ($D = 0.80474, P > 0.10; F_s = 1.811$), 2016 cpDNA sequences ($D = 1.38922, P > 0.10; F_s = 12.439$), and 2022 cpDNA sequences ($D = 2.2589, P < 0.05; F_s = 11.3$), but were negative for 2022 nrDNA sequences ($D = -1.18345, P > 0.10; F_s = -3.937$) (Table 2). These results indicate that our sequences (with the only exception of 2022 cpDNA) are in agreement with the null hypothesis of constant population size and neutral evolution. The hierarchical mismatch analysis showed the distributions of differences for all populations (Figure S3), from which the hypothesis of demographic population expansion can be rejected.

| Discussion 4.1 | Very quick effects of anthropogenic barriers on phylogeographical patterns The evaluation of the effects of habitat fragmentation on animal and plant species has been traditionally addressed by comparing gene flow, genetic differentiation, and genetic structure of populations on fragmented and non-fragmented habitats simultaneously (Chung et al., 2014a; Gao et al., 2015; Schlaepfer et al., 2018). For example, Su et al. (2003) compared the genetic differentiation of populations separated by the Great Wall of China with those not subjected to this huge physical separation for six plants, and found attributable differences to the presence of the wall during 600 years. On a second example, the levels of genetic divergence in two crayfishes (*Faxonius validus* and *Faxonius erichsonianus*) were significantly higher in streams impounded for 36–104 years than in non-impounded streams in Alabama, United States (Barnett et al., 2020). Direct comparisons (i.e. comparing before and after the fragmentation event the populations that have actually been subjected to such disturbance) are probably not available in the literature as it is assumed that the time elapsed from fragmentation should be very long, as enough generations should have passed to observe genetic changes. In their meta-analysis, Schlaepfer et al. (2018) found that effects are generally only observable after 50 years, although some exceptions could apply, as cases in which only 1–5 generations have passed. Herein we have measured the fragmentation effects of anthropogenic construction by using the same populations of a plant (*Primulina heterotricha*) two times within six years (i.e. two generations of the

study plant would have passed). We have detected a significant geographic structure in eight populations (Figures 2, 3), and AMOVA shows a high level of genetic variation between regions (Table 4), indicating significant genetic differentiation and limited gene flow among populations and regions. Both the phylogenetic tree and the STRUCTURE results indicated that there are three distinct genetic lineages, corresponding to three clades, i.e., northwest clade (NW region), southwest clade (SW region), and southeast clade (SE region) (Figures 2, 3). As one may expect for a species inhabiting a rugged mountain area (and where some rivers were dammed since the late 20th century), such a significant geographic structure was already detected before the expressway construction (2016). Although the effects are not still considerable (probably due to the insufficient time elapsed), we have been able to detect some changes in the genetic structure of *P. heterotricha* just a few years after the two expressways were completed. The three clades detected for *P. heterotricha* would likely predate the formation of the anthropogenic barriers of the Daguangba Reservoir and Expressways 1 and 2, as the range of this species, which occurs in mountains at relatively high elevations, is naturally fragmented by river valleys. As it can be observed in Fig. 1 (and Figures 4, 5), Expressway 1 has been constructed along the Changhua River (whose valley is, at some parts, up to 3 km wide) that crosses Hainan’s south-central mountain system in a SW–NE direction, and then the river turns into the NW, where it is dammed by the Daguangba Reservoir. Expressway 2 has been constructed taking advantage of the Tongshi River valley in spite of being much narrower. However, as our results show, the anthropogenic constructions would have intensified the isolation effects of the Changhua River and its associated valley, which has been cultivated since a long time ago (Xiao et al., 2012). In addition, conventional roads were built in these river valleys much earlier; for example, road G224, which was completed in 1954, runs nearly the same route as the two expressways. The changes in the significance of barriers before and after road construction in the BARRIER analysis (Figures 4, 5) suggest that geographic isolation caused by human constructions is key for understanding the present phylogeographical patterns of *P. heterotricha*. Most of the first barrier for both the nrDNA and cpDNA for the year 2016 corresponds to the separation between QX and WZ populations, which does not match with any of the anthropogenic constructions. In contrast, for the year 2022 the first barrier coincides with the dam and the expressways for both sequences. Another undisputable signal showing the important role of the anthropogenic barriers on the genetic structure of *P. heterotricha* is the sharp changes in the genetic affinities of population XA, both for nrDNA and cpDNA (Figure 3), which may be caused by the isolation of Expressway 1 but specially Expressway 2. Although it is hard to discern the relative contribution of valleys and rivers on one hand, and expressways on the other hand, the above-described changes in the generic partners from 2016 to 2022 suggest that the two expressways might contribute to shaping the phylogeographical patterns of the island-endemic *P. heterotricha* within six years, corresponding to two generations of the plant. Geographical discontinuity including anthropogenic disturbance is an important factor in population differentiation by weakening or blocking gene flow in many plant species (Slatkin, 1985; Su et al., 2003; Kartzinel et al., 2013; Chung et al., 2014b). These effects are even greater for small herbaceous plants like *P. heterotricha*, with a poor dispersal potential associated with small seeds dispersed largely by water.

4.2 | Effects of anthropogenic barriers on genetic structure

Although the different clades of *P. heterotricha* keep stable population dynamics, as revealed by mismatch distribution analysis (Figure S3), the plant would have suffered some detectable effects on its genetic structure, caused by the reduced exchange of genes. Notably, the sharing of ribotypes among the three groups of populations separated by the expressway network almost disappeared, and population genetic differentiation based on nrDNA increased both at the population level ($F_{ST[2016]} = 0.0045$, $F_{ST[2022]} = 0.0054$, $P < 0.01$) and at the region level (Table S3) from 2016 to 2022. In contrast, F_{ST} remained invariable along time with cpDNA at the population level (0.0098 in 2016 vs. 0.0097 in 2022; Table S2) and even increased at the group level (F_{ST} only decreased between NW and SE regions, which could be attributable to the Expressway 1 construction; Table S4). This incongruence between nrDNA and cpDNA could stem both from the different modes of inheritance of these two markers (nrDNA is biparentally inherited, cpDNA is only maternally inherited) and from the fact that pollen migration rates are often much higher than seed migration rates (Ennos, 1994; Petit et al., 2005). Thus, one could expect that the maternally-inherited cpDNA (which is only transmitted by seeds) would be much less sensitive to the fragmentation effects, particularly if we take into account that the anthropogenic barriers would have affected pollen flow in a much higher extent than

seed flow (see below).

Genetic differentiation was higher between populations separated by the dam than populations separated by the expressways (Tables S3, S4), i.e. the Daguangba Reservoir showed a more obvious and significant barrier effect on gene flow. Two factors could explain such an observed pattern. Firstly, the reservoir was built in 1994 and nearly a period of 30 years of isolation would have accumulated much more barrier effects on plant dispersal than the newly completed expressways, with a six-year period of effects or two generations of *P. heterotricha*. Secondly, the dam has a water reservoir of about 6 km long and a water surface of 100 km². Such physical impediment probably brings much more barrier effects than the expressways, which are normally only 20–30 m wide. For *P. heterotricha*, its seeds are small and may be largely dispersed by raindrops or water courses and its pollination needs small-sized insects such as *Amegilla leptocoma* and *A. yunnanensis* (Ling et al., 2017a). Such dispersal mechanisms would have been affected by the Daguangba Reservoir, as dams could restrict hydrochory (Andersson et al., 2000). Effects, however, would be much more pervasive regarding pollen dispersal, as the flying distances of these small insects would be hardly enough to connect the two banks of the reservoir (separated by up to 4 km).

Despite having less impact than the reservoir, the effects of expressways are still notable for *P. heterotricha*. In addition to the physical barrier posed by the two high-capacity roads, the rapid growth of traffic (especially after the end of the COVID-19 pandemic) with much more noise and accumulation of pollutants will increase the levels of disturbance. The fast-moving traffic and changes in wind conditions associated with expressways probably affected pollinator movements of *P. heterotricha* thus decreasing pollen flow. Negative effects of roads on the movement (and even survival) of pollinators have been often detected (Stephens et al., 2000; Bhattacharya et al., 2003; Baxter-Gilbert et al., 2015; Fitch & Vaidya, 2021; Dániel-Ferreira et al., 2022). Although road construction might change hydrological conditions (by affecting natural flow pathways and water quality, e.g. Buchanan et al., 2013), we have not been able to find examples in the literature of roads affecting hydrochory.

In conclusion, we provide evidence of the increased barrier effects of anthropogenic constructions such as reservoirs and expressways on genetic structure and phylogeographical patterns within just two generations of this plant. These disruptive effects involving habitat fragmentation may pose primary threats to population regeneration, genetic diversity, and change the evolutionary processes of plants, especially in endemic, threatened short-lived plants. To alleviate such negative pressure, we suggest establishing ecological corridors to enhance gene flow between populations separated by these anthropogenic barriers. These could include road tunnels and overpass woodlands, which enhance the dispersal of seeds, including the movement of insects and reptiles (such as lizards and frogs). Such ecological corridors might also increase the vegetation integrity and habitat continuity between the two sides of these barriers and thus be helpful for the long-term persistence of the island-endemic *P. heterotricha* and other rare and endangered species.

REFERENCES

- Almeida-Rocha, J. M., Soares, L. A. S. S., Andrade, E. R., Gaiotto, F. A., & Cazetta, E. (2020). The impact of anthropogenic disturbances on the genetic diversity of terrestrial species: A global meta-analysis. *Molecular Ecology*, 29(24), 4812–4822.
- Aguilar, R., Ashworth, L., Galetto, L., & Aizen, M. A. (2006). Plant reproductive susceptibility to habitat fragmentation: review and synthesis through a meta-analysis. *Ecology Letters*, 9(8), 968–980.
- Akaike, H. (1981). Likelihood of a model and information criteria. *Journal of Econometrics*, 16(1), 3–14.
- Andersson, E., Nilsson, C., & Johansson, M.E. (2000). Effects of river fragmentation on plant dispersal and riparian flora. *Regulated Rivers-research & Management*, 16, 83–89.
- Bhattacharya, M., Primack, R.B., & Gerwein, J. (2003). Are roads and railroads barriers to bumblebee movement in a temperate suburban conservation area. *Biological Conservation*, 109, 37–45.
- Barnett, Z.C., Adams, S.B., Ochs, C.A., & Garrick, R.C. (2019). Crayfish populations genetically fragmented

in streams impounded for 36–104 years. *Freshwater Biology* , 65, 768–785.

Baxter-Gilbert, J.H., Riley, J.L., Neufeld, C.J., Litzgus, J.D., & Lesbarrères, D. (2015). Road mortality potentially responsible for billions of pollinating insect deaths annually. *Journal of Insect Conservation* , 19, 1029–1035.

Berli, P., & Felsenstein, J. (2001). Maximum likelihood estimation of a migration matrix and effective population sizes in n subpopulations by using a coalescent approach. *Proceedings of the National Academy of Sciences of the United States of America* , 98(8), 4563–4568.

Buchanan, B., Easton, Z. M., Schneider, R. L., & Walter, M. T. 2013. Modeling the hydrologic effects of roadside ditch networks on receiving waters. *Journal of Hydrology* , 486, 293–305.

Chung, M. Y., Nason, J. D., López-Pujol, J., Yamashiro, T., Yang, B.-Y., Luo, Y.-B., & Chung, M. G. (2014a). Genetic consequences of fragmentation on populations of the terrestrial orchid *Cymbidium goeringii* . *Biological Conservation* , 170, 222–231.

Chung, M. Y., López-Pujol, J., & Chung, M. G. (2014b). Comparative genetic structure between *Sedum ussuriense* and *S. kamtschaticum* (Crassulaceae), two stonecrops co-occurrence on rocky cliffs. *American Journal of Botany* , 101(6), 946–956.

Crimmins, T. M., Crimmins, M. A., & Bertelsen, C. D. (2011). Onset of summer flowering in a 'Sky Island' is driven by monsoon moisture. *New Phytologist* , 191(2), 468–479.

Daniel-Ferreira, J., Berggren, A., Bommarco, R., Wissman, J., & Ockinger, E. (2022). Bumblebee queen mortality along roads increase with traffic. *Biological Conservation* , 272, 109634.

Deméou, B. B., Pineiro, R., & Hardy, O. J. (2016). Origin and history of the Dahomey Gap separating West and Central African rain forests: insights from the phylogeography of the legume tree *Distemonanthus benthamianus* . *Journal of Biogeography* , 43(5), 1020–1031.

Doyle, J. J., & Doyle, J. L. (1987). A rapid DNA isolation method for small quantities of fresh tissues. *Phytochemical Bulletin* , 19(1), 11–15.

Dong, W. P., Xu, C., Li, C. H., Sun, J. H., Zuo, Y. J., Shi, S., Cheng, T., Guo, J. J., & Zhou, S. L. (2015). *yef 1*, the most promising plastid DNA barcode of land plants. *Scientific Reports* , 5(1), 8348.

Duarte, G. T., Santos, P. M., Cornelissen, T. G., Ribeiro, M. C., & Paglia, A. P. (2018). The effects of landscape patterns on ecosystem services: meta-analyses of landscape services. *Landscape Ecology* , 33, 1247–1257.

Earl, D. A., & vonHoldt, B. M. (2012). STRUCTURE HARVESTER: a website and program for visualizing STRUCTURE output and implementing the Evanno method. *Conservation Genetics Resources* , 4(2), 359–361.

Ellwanger, C., Steger, L., Pollack, C., Wells, R., & Fant, B. J. (2022). Anthropogenic fragmentation increases risk of genetic decline in the threatened orchid *Platanthera leucophaea* . *Ecology and Evolution* , 12(2), e8578.

Ennos, R. A. (1994). Estimating the relative rates of pollen and seed migration among plant populations. *Heredity* , 72, 250–259.

Evanno, G. S., Regnaut, S., & Goudet, J. (2005). Detecting the number of clusters of individuals using the software STRUCTURE: a simulation study. *Molecular Ecology* , 14(8), 2611–2620.

Fitch, G., & Vaidya, C. (2021). Roads pose a significant barrier to bee movement, mediated by road size, traffic and bee identity. *Journal of Applied Ecology* , 58, 1177–1186.

Francisco-Ortega, J., Wang, Z. S., Wang, F. G., Xing, F. W., Liu, H., Xu, H., Xu, W. X., Luo, Y. B., Song, X. Q., Gale, S., Boufford, D. E., Maunder, M., & An, S. Q. (2010a). Seed Plant Endemism on Hainan Island: A Framework for Conservation Actions. *The Botanical Review* , 76, 346–376.

- Francisco-Ortega, J., Wang, F. G., Wang, Z. S., Xing, F. W., Liu, H., Xu, H., Xu, W. X., Luo, Y. B., Song, X. Q., Gale, S., Boufford, D. E., Maunder, M., & An, S. Q. (2010b). Endemic Seed Plant Species from Hainan Island: A Checklist. *The Botanical Review* , 76, 295–345.
- Gao, Y., Ai, B., Kong, H. H., Kang, M., & Huang, H. W. (2015). Geographical pattern of isolation and diversification in karst habitat islands: a case study in the *Primulina eburnea* complex. *Journal of Biogeography* , 42(11), 2131–2144.
- Haddad, N. M., Brudvig, L. A., Clobert, J., Davies, K. F., Gonzalez, A., Holt, R. D., ... Townshend, J. R. (2015). Habitat fragmentation and its lasting impact on Earth's ecosystems. *Science Advances* , 1(2), e1500052.
- Hall, T. A. (1999). BioEdit: A User-friendly Biological Sequence Alignment Editor and Analysis Program for Windows 95/98/NT. *Nucleic Acids Symposium Series* , 41, 95–98.
- Honnay, O., & Jacquemyn, H. (2007). Susceptibility of common and rare plant species to the genetic consequences of habitat fragmentation. *Conservation Biology* , 21(3), 823–831.
- Kartzinel, T. R., Shefferson, R. P., & Trapnell, D. W. (2013). Relative importance of pollen and seed dispersal across a Neotropical mountain landscape for an epiphytic orchid. *Molecular Ecology* , 22(24), 6048–6059.
- Kumar, S., Nei, M., Dudley, J., & Tamura, K. (2008). MEGA: A biologist-centric software for evolutionary analysis of DNA and protein sequences. *Briefings in Bioinformatics* , 9(4), 299–306.
- Laurance, W. F., Goosem, M., & Laurance, S. G. (2009). Impacts of roads and linear clearings on tropical forests. *Trends in Ecology & Evolution* , 24(12), 659–669.
- Lei, J. R., Chen, Z. Z., Chen, X. H., Li, Y. L., & Wu, T. T. (2020). Spatio-temporal changes of land use and ecosystem services value in Hainan Island from 1980 to 2018. *Acta Ecologica Sinica* , 40(14), 4760–4773. (In Chinese English Abstract)
- Li, Z. Y., & Wang, Y. Z. (2005). *Plants of Gesneriaceae in China* . Henan Science and Technology Publishing House.
- Li, Y., Zhai, S. N., Qiu, Y. X., Guo, Y. P., Ge, X. J., & Comes, H. P. (2011). Glacial survival east and west of the 'Mekong–Salween Divide' in the Himalaya–Hengduan Mountains region as revealed by AFLPs and cpDNA sequence variation in *Sinopodophyllum hexandrum* (Berberidaceae). *Molecular Phylogenetics and Evolution* , 59(2), 412–424.
- Ling, S. J., Meng, Q. W., Tang, L., & Ren, M. X. (2017a). Pollination syndromes of Chinese Gesneriaceae: a comparative study between Hainan Island and neighboring regions. *The Botanical Review* , 83, 59–73.
- Ling, S. J., Meng, Q. W., Tang, L., & Ren, M. X. (2017b). Gesneriaceae on Hainan Island: distribution patterns and phylogenetic relationships. *Biodiversity Science* , 25(8), 807–815. (In Chinese with English Abstract)
- Ling, S. J., Qin, X. T., Song, X. Q., Zhang, L. N., & Ren, M. X. (2020a). Genetic delimitation of *Oreocharis* species from Hainan Island. *PhytoKeys* , 157, 59–81.
- Ling, S. J., Guan, S. P., Wen, F., Shui, Y. M., & Ren, M. X. (2020b). *Oreocharis jasminina* (Gesneriaceae), a new species from mountain tops in Hainan Island, South China. *PhytoKeys* , 157, 121–135.
- Lowe, A. J., Cavers, S., Boshier, D., Breed, M. F., & Hollingsworth, P. M. (2015). The resilience of forest fragmentation genetics—no longer a paradox—we were just looking in the wrong place. *Heredity* , 115(2), 97–99.
- Long, W. X., Du, Y. J., Hong, X. J., Zang, R. G., Yang, Q., Xue, H. (2021). The experiences of Hainan Tropical Rainforest National Park pilot. *Biodiversity Science* , 29, 328–330. (In Chinese with English

Abstract)

- MacArthur, R. H., & Wilson, E. O. (1967). *The Theory of Island Biogeography*. Princeton University Press.
- Mantel, N. (1967). The detection of disease clustering and a generalized regression approach. *Cancer Research*, 27(2), 209–220.
- Manni, F., Guerard, E., & Heyer, E. (2004). Geographic patterns of (genetic, morphologic, linguistic) variation: How barriers can be detected by using Monmonier’s algorithm. *Human Biology*, 76(2), 173–190.
- Manoel, R. O., Rossini, B. C., Cornacini, M. R., Moraes, M. L. T., Cambuim, J., Alcantara, M. A. M., Silva, A. M., Sebbenn, A. M., & Marino, C. L. (2021). Landscape barriers to pollen and seed flow in the dioecious tropical tree *Astronium fraxinifolium* in Brazilian savannah. *PloS ONE*, 16(8), e0255275.
- Martinez-Ramos, M., Ortiz-Rodriguez, I. A., Pinero, D., Dirzo, R., & Sarukhan, J. (2016). Anthropogenic disturbances jeopardize biodiversity conservation within tropical rainforest reserves. *Proceedings of the National Academy of Sciences of the United States of America*, 113(19), 5323–5328.
- Moraes, M. A., Kubota, T. Y. K., Rossini, B. C., Marino, C. L., Freitas, M. L. M., Moraes, M. L. T., da Silva, A. M., Cambuim, J., & Sebbenn, A. M. (2018). Long-distance pollen and seed dispersal and inbreeding depression in *Hymenaea stigonocarpa* (Fabaceae: Caesalpinioideae) in the Brazilian savannah. *Ecology and Evolution*, 8(16), 7800–7816.
- Musher, L. J., Giakoumis, M., Albert, J., Del-Rio, G., Rego, M., Thom, G., Aleixo, A., Ribas, C. C., Brumfield, R. T., Smith, B. T., & Cracraft, J. (2022). River network rearrangements promote speciation in lowland Amazonian birds. *Science Advances*, 8(14), eabn1099.
- Myers, N., Mittermeier, R. A., Mittermeier, C. G., da Fonseca, G. A., & Kent, J. (2000). Biodiversity hotspots for conservation priorities. *Nature*, 403(6772), 853–858.
- Nualart, N., Herrando-Moraira, S., Cires, E., Guardiola, M., Laguna, E., Perez-Prieto, D., Saez, L., & Lopez-Pujol, J. (2021). Reusing old and producing new data is useful for species delimitation in the taxonomically controversial Iberian endemic pair *Petrocoptis montsicciana* / *P. pardoi* (Caryophyllaceae). *Diversity*, 13(5), 205.
- Nylander, J. A. A. (2004). *MrModeltest v2. Program distributed by the author*. Uppsala: Evolutionary Biology Centre, Uppsala University.
- Peakall, R., & Smouse, P. E. (2012). GenAlEx 6.5: genetic analysis in Excel. Population genetic software for teaching and research—an update. *Bioinformatics*, 28(19), 2537–2539.
- Petit, R. J., Duminil, J., Fineschi, S., Hampe, A., Salvini, D., Vendramin, G. G. (2005) Comparative organization of chloroplast, mitochondrial and nuclear diversity in plant populations. *Molecular Ecology*, 14, 689–701.
- Rambaut, A., & Drummond, A. J. (2007). Tracer v1.5. Available at: <http://beast.bio.ed.ac.uk/Tracer>.
- Rambaut, A. (2009). Figtree v.1.4.2. Available at: <http://tree.bio.ed.ac.uk/software/figtree>.
- Robin, V. V., Vishnudas, C. K., Gupta, P., & Ramakrishnan, U. (2015). Deep and wide valleys drive nested phylogeographic patterns across a montane bird community. *Proceedings of the Royal Society B: Biological Sciences*, 282(1810), 20150861.
- Rozas, J., Ferrer-Mata, A., Sanchez-DelBarrio, J. C., Guirao-Rico, S., Librado, P., Ramos-Onsins, S. E., & Sanchez-Gracia, A. (2017). DnaSP 6: DNA Sequence Polymorphism Analysis of Large Data Sets. *Molecular Biology and Evolution*, 34(12), 3299–3302.
- Ronquist, F., Teslenko, M., van der Mark, P., Ayres, D. L., Darling, A., Höhna, S., Larget, B., Liu, L., Suchard, M. A., & Huelsenbeck, J. P. (2012). MrBayes 3.2: Efficient Bayesian Phylogenetic Inference and Model Choice Across a Large Model Space. *Systematic Biology*, 61(3), 539–542.

- Schlaepfer, D. R., Braschker, B., Rusterholz, H., & Baur, B. (2018). Genetic effects of anthropogenic habitat fragmentation on remnant animal and plant populations: a meta-analysis. *Ecography* , 9, e02488.
- Slatkin, M. (1985). Gene flow in natural populations. *Annual Review of Ecology and Systematics* , 16(1), 393–430.
- Sork, V. L., & Smouse, P. E. (2006). Genetic analysis of landscape connectivity in tree populations. *Landscape Ecology* , 21, 821–836.
- Stephens, A. N., Roucou, X., Artika, I. M., Devenish, R. J., & Nagley, P. (2000). Topology and proximity relationships of yeast mitochondrial ATP synthase subunit 8 determined by unique introduced cysteine residues. *European journal of biochemistry* , 267(21), 6443–6451.
- Su, H., Qu, L. J., He, K., Zhang, Z., Wang, J., Chen, Z., & Gu, H. (2003) The Great Wall of China: a physical barrier to gene flow? *Heredity* , 90, 212–219.
- Swofford, D. L. (2002). PAUP*: Phylogenetic Analysis Using Parsimony, Version 4.0b10. Sunderland, MA: Sinauer.
- Taberlet, P., Gielly, L., Pautou, G., & Bouvet, J. (1991). Universal primers for amplification of three non-coding regions of chloroplast DNA. *Plant Molecular Biology* , 17(5), 1105–1109.
- Tambarussi, E.V., Boshier, D., Vencovsky, R., Freitas, M. L. M., & Sebbenn, A. M. (2017). Inbreeding depression from selfing and mating between relatives in the Neotropical tree *Cariniana legalis* Mart. Kuntze. *Conservation Genetics* , 18, 225–234.
- Trombulak, S. C., & Frissell, C. A. (2000). Review of ecological effects of roads on terrestrial and aquatic communities. *Conservation Biology* , 14(1), 18–30.
- Vaidya, G., Lohman, D. J., & Meier, R. (2011). SequenceMatrix: concatenation software for the fast assembly of multi-gene datasets with character set and codon information. *Cladistics* , 27(2), 171–180.
- Wei, Y. G., Zhong, S. H., & Wen, H. Q. (2004). Studies of the flora and ecology Gesneriaceae in Guangxi Province. *Acta Botanica Yunnanica* , 26, 173–182. (In Chinese with English Abstract)
- Wei, Y. G. (2010). *Gesneriaceae of South China* . Guangxi Science and Technology Publishing House.
- White, T. J., Bruns, T. D., Lee, S. B., & Taylor, J. (1990). Amplification and Direct Sequencing of Fungal Ribosomal RNA Genes for Phylogenetics. *PCR Protocols* , 1990, 315–322.
- Xiao, Ming., Wu, J., Chen, Q., Jin, M., Hao, X., & Zhang, Y. (2012). Dynamic change of land use in Changhua downstream watershed based on CA-Markov model. *Nongye Gongcheng Xuebao. Transactions of the Chinese Society of Agricultural Engineering* , 28, 231–238. (In Chinese with English Abstract)
- Yang, X. B. (2013). *Flora of Hainan* . Science Press.
- Yao, X. L., Zhou, L., Wu, T. X., & Ren, M. X. (2022). Landscape dynamics and ecological risk of the expressway crossing section in the Hainan Rainforest National Park. *Acta Ecologica Sinica* , 42 (16), 6695–6703. (In Chinese with English Abstract)
- Young, A., Boyle, T., & Brown, T. (1996). The population genetic consequences of habitat fragmentation for plants. *Trends in ecology & evolution* , 11(10), 413–418.
- Zhao, Y., Vrieling, K., Liao, H., Xiao, M., Zhu, Y., Rong, J., Zhang, W., Wang, Y., Yang, J., Chen, J., & Song, Z. (2013). Are habitat fragmentation, local adaptation and isolation-by-distance driving population divergence in wild rice *Oryza rufipogon* ? *Molecular Ecology* , 22(22), 5531–5547.

Biosketch

Wen-Ting Jin and Shao-Jun Ling are interested in phytogeography and this work represents a component of their work respectively as a master and PhD student at Hainan University. They and the other authors collaborate on questions of island biodiversity and molecular biogeography based on international collaborations (see TBLab, www.tbcs.org).

Author contributions: Ming-Xun Ren and Jordi Lopez-Pujol conceived the ideas; Wen-Ting Jin and Shao-Jun Ling conducted the fieldwork and collected the data; Wen-Ting Jin, Shao-Jun Ling, and Ming-Xun Ren analysed the data. Wen-Ting Jin and Shao-Jun Ling wrote the first draft of the manuscript. Myong Gi Chung, Jordi Lopez-Pujol, Mi Yoon Chung, and Ming-Xun Ren extensively revised it. All authors read and reviewed the final manuscript.